

THEORETICAL STUDY OF THE 100 MeV LINAC, INJECTOR OF THE SR RING SOLEIL

M.-A.Tordeux, LURE-CNRS, Centre Universitaire Paris-Sud, F - 91898 Orsay Cedex, France
C. Bourat, THOMSON-CSF, Airsys HEA, F - 91195 Saint-Aubin Cedex, France

Abstract

A 100 MeV Linac will be built, in order to inject into the booster synchrotron of SOLEIL. Two modes of operation will be provided corresponding to single and multibunch modes of filling the storage ring. Calculation of the beam dynamics has been carried out from the gun to the injection point into the Booster. Special care has been taken so that no noticeable change needs to be made between the two running modes, as well as in the reliability and the economical aspects of the injector. Two different numerical codes have been used, providing space charge calculations : PARMELA [1] and DYPAL (Thomson-CSF). Comparisons of the results will be presented.

1. INTRODUCTION

The beam dynamics of the whole injector was studied using different numerical codes. However, special attention will be given to the calculations made with the DYPAL code (Thomson), and comparisons will be made with the PARMELA code [1].

DYPAL solves the Lorentz equation equivalent to a first order differential system with 6 equations :

$$\frac{d\mathbf{p}}{dt} = q\mathbf{E} + q\mathbf{v} \times \mathbf{B}. \text{ The independent variable is time.}$$

The differential system is solved with the Hamming method [2], a 4th order predictor-modifier-corrector method (PMC). The step is variable according to the truncation error. Various external electromagnetic fields \mathbf{E} , \mathbf{B} can be applied, such as accelerating fields in cavities (paraxial approximation), including traveling wave fields, focusing solenoidal and multipolar transverse fields. The space charge is evaluated with a relativistic 3D particle-particle method (PP). The relevant fields applied to a charge j by a charge i are:

$$\mathbf{E}_i = \frac{\gamma_i q_i}{4\pi\epsilon_0} \frac{\mathbf{r}_{ij}}{[\mathbf{r}_{ij}^2 + (\mathbf{r}_{ij} \cdot \gamma_i \boldsymbol{\beta}_i)^2]^{3/2}} \quad c\mathbf{B}_i = \boldsymbol{\beta}_i \times \mathbf{E}_i$$

To avoid fictional collision problems, a "cut-off" distance R_c is computed according to spatial statistics and modifies the Coulomb law at short distances.

2. TECHNICAL SPECIFICATIONS AND GENERAL LAY-OUT OF THE LINAC

Figure 2.1. shows a schematic lay-out of the 100 MeV linac : it consists of a 90 kV gun, 3 short focusing lenses between the gun and the buncher, a harmonic prebuncher at 2 998 MHz, a 15 MeV standing wave buncher, and finally two accelerating traveling wave structures giving an energy of 2 x 42.5 MeV.

The main specifications of the injector are presented elsewhere [3], and consist of two running modes : a long pulse train of 300 ns/1.6 nC at 12 Hz ensuring the high brilliance injection mode, and the short pulse 2ns/0.2 nC at 12 Hz providing temporal structure injection mode. As a result, two current levels are required at the gun anode : 30 mA and 300 mA.

3. SIMULATION RESULTS FOR THE LINAC

3.1. The gun and the prebunching process

Geometries of the wehnelt and anode electrodes are chosen to deal with the range of beam current. The EGUN code is used for this optimization. The cathode will be an EIMAC Y-845 with a 0.5 cm² emissive area. The geometry is in fact optimal for about 150-200 mA with a minimum emittance. For both operation modes at 30 mA and 300 mA, the un-normalized emittances are estimated as 10 π mm.mrad, with an adequate safety margin including thermal velocities and grid effects. However, no noticeable sensitivity of the final emittance to gun emittance has been found.

A prebunching cavity at 2 998 MHz is set at about 3.2 λ_0 upstream of the buncher. Its geometry is such that multipactor risks are minimized, thanks to noses and rounded shapes without opposing plane surfaces. Parameters are presented in Table 3.1. The beam modulation is about ± 9 -10 keV. In the 30 mA mode, the prebunching process compresses 61 % of the gun current inside 50° of phase extension, while in the 300 mA mode, 60 % of the gun current lies inside 70° of phase at the buncher input.

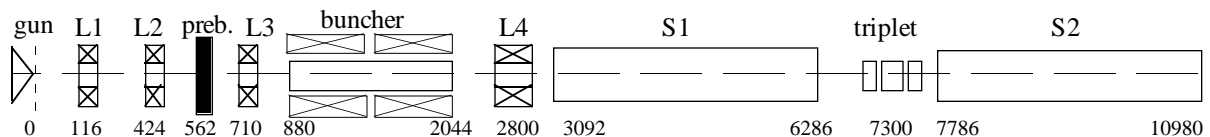


Figure 2.1. Schematic lay-out of the 100 MeV linac (unit in mm).

Table 3.1.

Prebunching Cavity, Bunching and accelerating section			
	<i>Prebuncher</i>	<i>Buncher</i>	<i>1 Section</i>
L between RF axis :	70 mm	1.1 m	3.070 m
Shunt impedance : (80 % superfish)	1.1 MΩ [Z]	40.2 MΩ/m [ZT ²]	61 MΩ/m [ZT ²]
Q ₀ quality fact. : (80 % superfish)	9 200	15 000	12 700
E ₀ average :	0.18 MV/m /0.19	18.7 MV/m	16.1 MV/m
P dissipated : (% saf. marg.)	90 W (20 %)		
Input power :		5 MW	17 MW
Energy gain :	-	15.7 MeV	48 MeV (I=0)

3.2. The bunching process

The buncher is a standing wave structure at the $\pi/2$ mode. The beam aperture diameter is ϕ 27 mm. The first two of the 22 cells have a reduced beta for the bunching process ($\beta = 0.78$ and 0.90). Structure parameters are shown in Table 3.1.

Concerning beam focalisation, two long shielded solenoids surround the buncher section, providing a maximum field of 0.15 T. Note that only the first will be powered at 0.11 T for the nominal working point. In that condition, the beam is theoretically divergent at the buncher exit, and therefore permits efficient control by the shielded lens which is placed before the first accelerating section.

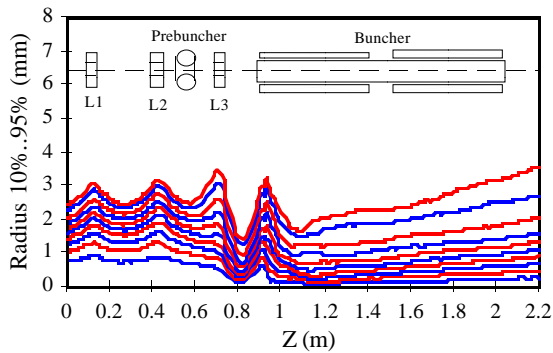


Figure 3.1. 300 mA mode - DYPAL code.

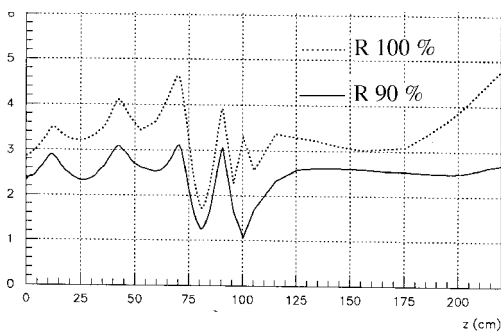


Figure 3.2. 300 mA mode - PARMELA code.

Calculations for the 30 mA (resp. 300 mA) mode give 65.3 % (resp. 58 %) of the gun current inside 13.5° of phase extension at buncher exit. 66 % of the 30 mA gun current lies in ± 0.4 % energy spread, while 59 % of the 300 mA gun current lies in ± 0.64 % energy spread. Figures 3.1. and 3.2. compare the beam envelopes from the gun to the buncher output, with the DYPAL and PARMELA codes.

3.3. The RF accelerating sections

The main accelerating waveguides are standard traveling wave $2\pi/3$ mode sections, designed with a constant gradient for zero current. The beam aperture varies from ϕ 22.6 mm to ϕ 17 mm, giving a group velocity c/v_g from 52.3 to 136.2, over 92 cells plus 2 1/2 RF coupling cells. The filling time is 840 ns and the power attenuation is 5.1 dB. In the beam dynamics simulations, the 16.1 MV/m average field gives an energy of 110 MeV at the end of the linac. See Table 3.1. for further parameters.

The sections are used without external focusing, except for a triplet between them. The optimal settings are such that waists are obtained in the middle of each section.

Table 3.2.

Beam properties for $I_{anode} = 30$ and 300 mA injection mode		
<i>injection mode :</i>	<i>multibunch</i>	<i>single bunch</i>
Final average energy	110 MeV	110 MeV
Total current transm.	76.4 %	73.8 %
Current transm. in :		
$\Delta\phi = 15^\circ$	66 % (20 mA)	60 % (179 mA)
$\Delta E/E = \pm 0.6$ %	63 % (19 mA)	56 % (168 mA)
$\Delta E/E = \pm 0.14$ %	43 % (13 mA)	47 % (140 mA)
$4\beta\gamma\sigma' = 49.9 \pi 10^{-6}$ mrad (energy filter)	57 % (17 mA) (± 1.5 %)	
$4\beta\gamma\sigma' = 155 \pi 10^{-6}$ mrad (energy filter)		48 % (144 mA) (± 0.6 %)

Table 3.2. gives the beam properties for both main operation modes at 30 mA and 300 mA. Figure 3.3. shows the phase space diagram at the end of the linac in 300 mA mode.

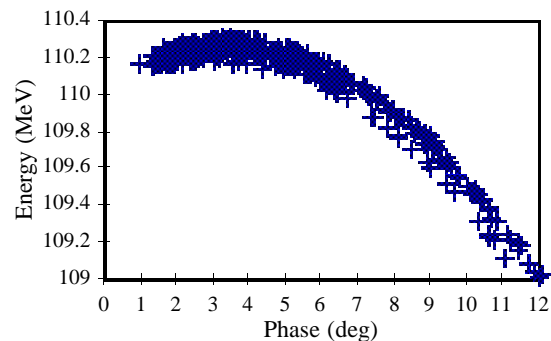


Figure 3.3. Phase space diagram at 110 MeV (300 mA mode).

4. TRANSFER LINE TO THE BOOSTER

The aim of the transfer line is to inject the beam on-axis into the booster, with an energy spread of $\pm 1.5\%$ around the mean energy. Optical and dispersion functions have to coincide at the septum exit, for both the injected and stored beam. The admittance of the line has to be more or less equal to the emittance which is vertically accepted in the booster, that is $10^{-6} \pi$ m.rad un-normalized.

4.1 Magnets : types and tolerances

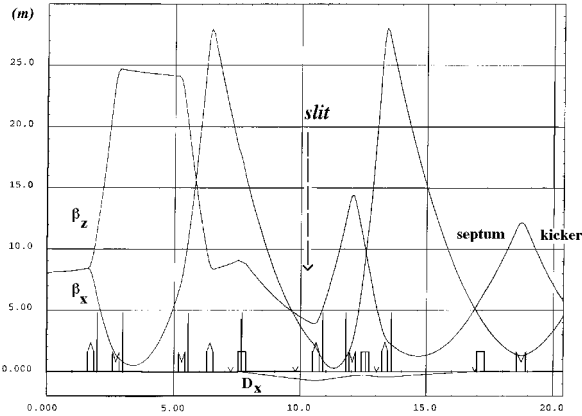


Figure 4.1. Optical functions from Linac until injection point into the Booster (BETA-LNS code).

The optical functions through the line are shown in Fig. 4.1. A complete lay-out of the transport can be found elsewhere [3].

One can see the first split triplet for beam matching, which tuning allows to optimize the slit resolution (0.5%). Thereafter, two dipoles, three more quadrupoles and the septum magnet achieve the double achromaticity together with the required optical functions. Quadrupole gradients do not exceed 1 T/m @ 25 cm for a 100 MeV beam. Dipole characteristics are presented in Table 4.1.

Table 4.1.

Transfer Line Dipoles characteristics				
	type	aperture (HxV mm ²)	Lmag (m)	ρ at 100 MeV (m)
D1=D2	solid rectangular	120x36	0.3	1.1459
septum	eddy current passive copper	18x15	0.3	2.2918

We defined the tolerances for the reproducibility of the dipole field and quadrupole gradient, using the BETA-LNS code [4]. Multipolar components of magnets were examined using the TURTLE code [5], which calculates second-order geometrical optics, and all-order chromatic optics in quadrupoles and multipoles.

Finally, we imposed less than 10% variation for the optical functions at the end of the line, and 10% growth

for the vertical and horizontal statistical emittances. Table 4.2. shows the results.

Table 4.2.

Transfer Line Magnet tolerances		
	$\frac{\Delta \int Bdl}{\int Bdl}$	$\frac{\Delta \int Gdl}{\int Gdl}$
reproducibility :	(D1/2) $5 \cdot 10^{-4}$	(Q) $5 \cdot 10^{-3}$
multipolar (S)	(D1/2) $2 \cdot 10^{-3}$ at 17 mm	(Q) $3 \cdot 10^{-3}$ at 15 mm
component :	(septum) $3 \cdot 10^{-3}$ at 7.5 mm	

4.2. Injection mode into the booster

The septum magnet is an eddy current passive copper magnet, standardized with the extraction magnet from the booster. The 25 μ sec half-sine form current pulse is induced by a capacitive discharge at 12 Hz [6]. Another kicker provides the last impulse (12 mrad) before single pulse acceleration.

4.3. Tuning procedures

The dipolar correction procedure is made via 3 steerer pairs H, V with 4 aluminium-oxide screens. In addition, the two dipoles incorporate correction windings. A value of 0.25 mrad in the steerers maintains the excursion of the orbit below 0.3 mm (1σ) and this, for a standard misalignment of the magnets and screens equal to 0.2 mm in transverse plans and 0.5 mrad in rotation (1σ).

Besides, an emittance measurement in the straight line behind the first dipole is foreseen, using the three gradients method. It will allow the tuning of the matching section at the entrance of the line.

Special care has been taken for shielding against gamma and neutron radiation during spectrum measurements. An in-vacuum retractable graphite and lead beamcatcher is therefore installed before the septum magnet.

7 REFERENCES

- [1] PARMELA code, v5.03 of Orsay implementation by B. Mouton, LAL-SERA 97-85, 2nd April 1997.
- [2] "Mathematical methods for Digital Computers", A. Ralston and H. Wilf Eds., New York : Wiley (1960).
- [3] "Present design of ELIOS electron linac injector of SOLEIL SR ring", R. Chaput and al., this conference.
- [4] BETA-LNS code v5.0, J. Payet, CEA Saclay-L.N.S.
- [5] TURTLE code, D.C. Carey *FNAL*, K.L. Brown *SLAC*, C. Iselin *CERN*, March 1982.
- [6] *Pulsed Power Supply Workshop*, Daresbury, 23th March 1998.